

1 **A novel ultrasound-guided mouse model of sudden cardiac arrest**

2 Cody A. Rutledge¹, Takuto Chiba^{2,3}, Kevin Redding¹, Cameron Dezfulian⁴, Sunder Sims-Lucas^{2,3}, Brett A.
3 Kaufman¹

4

5 1. Division of Cardiology, Cardiovascular Institute, University of Pittsburgh, Pittsburgh, PA, USA

6 2. Rangos Research Center, Children's Hospital of Pittsburgh, University of Pittsburgh, Pittsburgh, PA,
7 USA

8 3. Division of Nephrology, Department of Pediatrics, University of Pittsburgh School of Medicine,
9 Pittsburgh, PA, USA.

10 4. Safar Center for Resuscitation Research and Critical Care Medicine Department, University of
11 Pittsburgh, Pittsburgh, PA, USA

12

13 Corresponding Author:

14 Brett Kaufman (bkauf@pitt.edu)

15

16 **Abstract**

17 *Aim:* Mouse models of sudden cardiac arrest are limited by challenges with surgical technique and
18 reliable venous access. To overcome this limitation, we sought to develop a simplified method in the
19 mouse that uses ultrasound-guided injection of potassium chloride directly into the heart.

20 *Methods:* Potassium chloride was delivered directly into the left ventricular cavity under ultrasound
21 guidance in intubated mice, resulting in immediate asystole. Mice were resuscitated with injection of
22 epinephrine and manual chest compressions and evaluated for survival, body temperature, cardiac
23 function, kidney damage, and diffuse tissue injury.

24 *Results:* The direct injection sudden cardiac arrest model causes rapid asystole with high surgical survival
25 rates and low surgical duration. Sudden cardiac arrest mice with 8-min of asystole have significant
26 cardiac dysfunction at 24 hours and high lethality within the first seven days, where after cardiac
27 function begins to improve. Sudden cardiac arrest mice have secondary organ damage, including
28 significant kidney injury, but no clear evidence of neurologic dysfunction.

29 *Conclusions:* Ultrasound-guided direct injection of potassium chloride allows for rapid and reliable
30 cardiac arrest in the mouse that mirrors human pathology. This technique lowers the barriers to entry
31 for adoption of the mouse model of sudden cardiac arrest, which will improve investigators' ability to
32 study the mechanisms underlying post-arrest changes.

33 **Introduction**

34 Out of hospital cardiac arrest affects over 350,000 patients annually in the United States¹. Only 10% of
35 these patients will survive to hospital discharge and only 6% of the patients will be discharged with a
36 favorable outcome^{2,3}. These statistics suggest a dramatic need for novel interventions to improve
37 cardiac arrest outcomes. Numerous animal models of sudden cardiac arrest (SCA) have been developed
38 to help understand the mechanisms underlying cardiac arrest mortality and to explore potential
39 interventions in pre-clinical models^{4,5}. A review of animal models of SCA found that only 6% of pre-
40 clinical SCA studies were completed in mice⁵. A mouse model has a number of advantages over large
41 animal models, including rapid breeding, cost-effectiveness, and opportunity for genetic manipulation.⁶
42 However, mouse use to model SCA has been limited by difficulty obtaining venous access and delivering
43 life support related to the animal's size^{7,8}.

44 The major limitation to adoption of the mouse model is the difficult cannulation of the delicate femoral
45 or internal jugular (IJ) veins, resulting in prolonged surgical times and high lethality. Moreover, venous
46 cannulation requires ligation of the vessel post-operatively, which may further contribute to organ
47 damage and alter outcomes. In this paper, we describe a novel method for ultrasound-delivery of
48 potassium chloride (KCl) directly into the left ventricle (LV) to induce immediate cardiac arrest,
49 bypassing the need for establishing intravenous access. This direct cardiac injection method simplifies
50 the surgical process, lowering the barrier to entry for this model. Our model has rapid procedure times
51 and high rate of surgical survival, thereby increasing the opportunity for study of preventative and
52 therapeutic interventions, as well as mechanistic aspects of organ damage and recovery.

53

54

55 **Methods**

56 **Animal Preparation**

57 8-week-old C57BL/6J male and female mice were anesthetized using 5% isoflurane in 100% oxygen via
58 induction box until reaching the surgical plane. These mice were placed in a supine position and
59 intubated by 22 g catheter and mechanically ventilated (MiniVent, Harvard Apparatus, Holliston, MA) at
60 a rate of 150 bpm (125 μ L for females and 140 μ L for males). Animal temperature was maintained near
61 37 °C via heating pad and rectal temperature probe and heart rate (HR) was monitored continuously
62 using surface electrocardiogram (ECG; Visual Sonics, Toronto, Canada). HR was maintained between
63 400-500 bpm by adjusting isoflurane concentration. Depilatory cream was applied to the thorax and the
64 chest cleaned with alcohol. All studies were performed at the University of Pittsburgh in compliance
65 with the National Institutes of Health Guidance for Care and Use of Experimental Animals and was
66 approved by the University of Pittsburgh Animal Care and Use Committee (Protocol #18032212).

67 **Ultrasound-guided KCl Delivery and Cardiopulmonary Resuscitation (CPR).**

68 Baseline transthoracic echocardiography was performed using the Vevo 3100 imaging systems (Visual
69 Sonics) with a 40 MHz linear probe along the long-axis of the heart. A 30-gauge needle was carefully
70 advanced under ultrasound-guidance through the intercostal space and directed into the LV (Figure 1A).
71 40 μ L of 0.5M KCl in saline was delivered into the LV cavity, causing immediate asystole on ECG. The
72 ventilator was turned off at this time. Doppler imaging was utilized over the aortic outflow tract to
73 confirm that no blood was ejected during asystole. The mice remained in asystole for 7.5 minutes, when
74 a second 30-gauge needle was introduced into the LV and 500 μ L of 15 μ g/mL epinephrine in saline was
75 delivered over approximately 30 seconds. At 8 minutes, the ventilation was resumed at 180 bpm and
76 CPR initiated. CPR was performed manually at 300 bpm for 1 min, at which time CPR was briefly held
77 and ECG evaluated for recovery of spontaneous circulation (ROSC). If a ventricular rhythm was observed
78 on ECG, doppler imaging was performed to confirm blood flow. If not, one to two additional 1-minute
79 cycles of CPR were performed. Animals not achieving ROSC by 3 minutes were euthanized. Mice
80 remained on the ventilator (without isoflurane) for approximately 20-25 minutes until breathing
81 spontaneously at a rate over 60 respirations/minute. Sham mice received no KCl injection, but did
82 receive a single direct LV injection of 500 μ L epinephrine and were extubated immediately after
83 injection. All animals were placed in a recovery cage under heat lamp for 2 hours with hourly
84 temperature monitoring for up to 4 hours. Survival was assessed every morning for a 4-week survival
85 cohort.

86 **Figure 1. Direct LV Injection Model of SCA.** A) Representative long-axis ultrasound image depicting
87 introduction of a needle into the LV chamber. B) Representative ECG tracings at baseline, during KCl
88 injection, during asystole, immediately after ROSC is achieved, and during recovery. C) Depiction of time
89 course of SCA in this model. D) Temperature monitoring in sham and arrest mice at baseline, time of
90 ROSC, and at 1, 2, 3, 4 and 24 hours post ROSC. Arrest mice have significantly depressed body
91 temperature at 3, 4, and 24 hours after arrest when compared to sham mice. E) Mortality curve
92 demonstrating decreased survival in arrest mice as compared to sham (initial sham n=5; arrest n=13).
93 Data are expressed as mean +/- SEM. * $=p < 0.05$

95 **Ultrasound and Echocardiography**

96 Echocardiography was performed at baseline, 1 day, 1 week, and 4 weeks as previously described¹⁴.
97 Briefly, transthoracic echocardiography was performed using the Vevo 3100 system and analyzed using
98 VevoLab v3.2.5 (Visual Sonics). B-mode images were taken for at least 10 cardiac cycles along the
99 parasternal long axis of the LV and end-systolic volume (ESV) and end-diastolic volumes (EDV) calculated
100 by modified Simpson's monoplane method¹⁵. Short-axis M-mode images were obtained at the level of
101 the papillary muscle for representative images only. Ejection Fraction (EF) was calculated from long-axis
102 B-mode imaging as: $100 \times (LV\ EDV - LV\ ESV) / (LV\ EDV)$.

103 A cohort of mice were assessed for renal perfusion following ROSC. The ultrasound probe was oriented
104 transversely across the abdomen at the plane of the right kidney. Doppler imaging over the renal artery
105 evaluated the presence of blood flow every thirty seconds until sustained blood flow was noted.

106 **Serum Analysis**

107 After euthanasia, mice underwent cardiac puncture for collection of blood by heparinized syringe. Blood
108 was separated by centrifugation at 2000 x g at 4 °C for 10 minutes and the serum was flash frozen.
109 These samples were evaluated for blood urea nitrogen (BUN), serum creatinine, alanine
110 aminotransferase (ALT), and creatine kinase (CK) by the Kansas State Veterinary Diagnostic Laboratories
111 (Manhattan, KS).

112 **Tissue Histology**

113 Kidneys were fixed overnight in 10% formalin at 4 °C then washed with PBS and transferred to 70%
114 ethanol at room temperature. After fixation, tissues were embedded into paraffin prior to sectioning at
115 4 microns by the Histology Core at the Children's Hospital of Pittsburgh. Sections were stained with
116 hematoxylin and eosin (H&E). Renal tubular pathology was semi-quantitatively scored (0: no injury to 4:
117 severe injury) in terms of tubular dilatation, formation of proteinaceous casts, and loss of brush
118 border¹⁶. Histological scoring was performed in a blinded fashion at 40x magnification on outer
119 medullary regions of the tissue sections. Eight fields were evaluated per sample. Samples were imaged
120 using a Leica DM 2500 microscope (Leica, Wetzlar, Germany) and LAS X software (Leica).

121 **Statistical Analysis**

122 Data were expressed and mean ± standard error in all figures. $p \leq 0.05$ was considered significant for all
123 comparisons. To determine whether sample data has been drawn from a normally distributed
124 population, D'Agostino-Pearson test was performed. For parametric data, Student's t-test was used to
125 compare two different groups. For nonparametric data, Mann-Whitney test was used. Survival analysis
126 was assessed by using Kaplan-Meier and log rank (Mantel-Cox) testing. All statistical analysis was
127 completed using Graphpad Prism 8 software (San Diego, CA).

128

129 **Results**

130 **Baseline sex, weight, EF and HR are similar between groups**

131 19 sham and 30 arrest mice were initially utilized in this study. There was no difference in baseline
132 weight (sham: 22.6 ± 0.9 g; arrest: 23.1 ± 0.6 g, Table 1), EF (sham: $59.8 \pm 1.5\%$; arrest: $59.9 \pm 1.0\%$) or HR
133 (sham: 472 ± 19 bpm; arrest: 488 ± 11 bpm) between groups. A single mouse from the sham group (1/19,
134 5.2%) and five mice from the arrest group (5/30, 16.7%) did not achieve ROSC or died immediately after
135 extubation. Arrest mice required an average of 1.32 minutes of CPR to achieve ROSC and were
136 extubated after an average of 22.7 minutes (Table 1). The distribution of males and females are similar
137 between groups (sham: 10 female, 9 male; arrest: 14 female, 16 male). While this study was not
138 powered to examine sex-based changes amongst groups, surgical survival was not biased by sex
139 distribution (Table 1).

140 **Table 1. Physiologic and Surgical Characteristics of Sham and SCA Mice**

	Sham (\pm SEM)	Arrest	p-value
Age (d)	56.8 ± 0.7 (n=18)	57.7 ± 0.6 (n=25)	0.34
Weight (g)	22.6 ± 0.9 (n=15)	23.1 ± 0.6 (n=25)	0.63
Sex	10 female, 9 male	14 female, 16 male	n/a
<u>Surgical Survival</u>			
Total	18/19	25/30	n/a
Males	9/9	14/16	
Females	9/10	11/14	
CPR Duration	n/a	1.32 ± 0.11 (n=25)	n/a
Time to Extubation	n/a	22.7 ± 0.7 (n=25)	n/a
Initial Body Temp (°C)	35.7 ± 0.2 (n=15)	35.5 ± 0.2 (n=25)	0.79
ROSC Body Temp (°C)	n/a	35.2 ± 0.2 (n=25)	n/a
1 h Body Temp (°C)	35.9 ± 0.1 (n=7)	35.9 ± 0.3 (n=14)	0.95
2 h Body Temp (°C)	35.8 ± 0.1 (n=7)	35.2 ± 0.3 (n=13)	0.18
3 h Body Temp (°C)	35.8 ± 0.1 (n=6)	33.0 ± 0.6 (n=9)	<0.001
4 h Body Temp (°C)	35.8 ± 0.1 (n=6)	32.9 ± 0.1 (n=5)	<0.001
24 h Body Temp (°C)	36.6 ± 0.2 (n=7)	34.8 ± 0.4 (n=10)	0.03
Baseline HR (bpm)	472 ± 19 (n=13)	488 ± 11 (n=19)	0.45
Baseline EF (%)	59.8 ± 1.5 (n=14)	59.9 ± 1.0 (n=19)	0.94

1 d HR (bpm)	521±18 (n=14)	459±12 (n=21)	0.007
1 d EF (%)	59.6±1.7 (n=14)	39.9±3.0 (n=21)	<0.001
1 wk EF (%)	59.6±2.3 (n=5)	41.4±3.4 (n=6)	0.002
4 wk EF (%)	59.5±2.6 (n=5)	49.8±5.3 (n=6)	0.4

141

142 **SCA mice have temperature and HR dysregulation after ROSC**

143 There were no significant differences in body temperature between groups at baseline (sham: 35.7±0.2
144 °C; arrest: 35.5±0.2 °C) (Table 1, Figure 1). Following extubation, mice were kept in a warmed recovery
145 cage, and no difference was noted at 1 hour (sham: 35.9±0.1 °C; arrest: 35.9±0.3 °C) or 2 hours (sham:
146 35.8±0.1 °C; arrest: 35.2±0.3 °C). Arrest mice had significantly lower body temperatures once removed
147 from the warming cage at 3 hours (sham: 35.8±0.1 °C; arrest: 33.0±0.6 °C, p<0.001), 4 hours (sham:
148 35.8±0.1 °C; arrest: 32.9±0.1 °C, p<0.001) and 24 hours (sham: 36.6±0.2 °C; arrest: 34.8±0.4 °C, p=0.03).
149 Arrest mice also had significantly lower HR one-day after SCA (sham 521±18 bpm; arrest 459±12 bpm,
150 p=0.007).

151 **SCA mice have increased 30-day mortality**

152 Of the post-operative survivors, a cohort from each group was evaluated for survival over a 4-week time
153 course. At 24 hours, 100% of sham mice survived (5 of 5) compared to 92% of arrest mice (12 of 13,
154 p=0.54). At 72 hours, 100% of sham mice were alive (5 of 5) compared to 46% of arrest mice (6 of 13,
155 p=0.052 vs sham). At 4 weeks, 100% of sham mice survived (5 of 5, median survival 28 days) compared
156 to only 38% of arrest mice (5 of 13, median survival 3 days, p=0.03; Figure 1). All of the SCA mouse
157 deaths occurred within seven days following arrest.

158 **SCA mice have reduced EF, which improves over time**

159 Sham and arrest mice showed no difference in baseline EF (sham: 59.8±1.5%; arrest: 59.9±1.0%). One
160 day after arrest, there was a significantly depressed EF in the arrest group (sham: 59.6±1.7%; arrest:
161 39.9±3.0%, p<0.001; Figure 2). EF of arrest mice remained significantly depressed 1 week after SCA
162 procedure (sham: 59.6±2.3%; arrest: 41.4±3.4%, p=0.002). Four weeks after arrest, there is no
163 significance between EF of sham and SCA groups (Figure 2).

164 **Figure 2. Ejection Fraction and Heart Rate in Sham and SCA Mice.** A) Representative M-mode tracings
165 of a sham (top) and arrest (bottom) mouse one day after SCA, where red lines denote LV width during
166 diastole and green lines denote systole. B) Heart rate (HR) and ejection fraction (EF) are similar between
167 groups at baseline, but significantly depressed in SCA mice compared to sham at 1 day after arrest. C) EF
168 is significantly decreased in SCA mice compared to sham at matched timepoints at 1 day and 1 week, but
169 there is no significant EF change by 4 weeks. Data are expressed as mean +/- SEM. P-values: *< 0.05, **
170 < 0.01, ***< 0.001.

171 **SCA mice have evidence of prolonged ischemia after SCA and kidney damage at one day**

172 As kidney damage is a common side effect of cardiac injury¹⁷, we evaluated the duration of renal
173 ischemia following SCA. A cohort of arrest mice (n=10) were evaluated for kidney reperfusion following

174 ROSC by evaluating renal artery flow. The mean duration of kidney ischemia was 20.6 minutes, with
175 initial measurable kidney blood flow occurring on average 11.3 minutes after ROSC (Figure 3). Serum
176 creatinine was significantly elevated in arrest mice at 1 day when compared to sham (sham: 0.36 ± 0.06
177 mg/dL; arrest: 1.52 ± 0.22 mg/dL, $p < 0.001$; Figure 3), as was serum BUN (sham: 21.5 ± 9.9 mg/dL; arrest:
178 156.0 ± 39.8 mg/dL, $p = 0.005$). Semi-quantitative scoring of tubular injury was performed at the outer
179 medulla and was noted to be higher in arrest mice (sham: 0.15 ± 0.05 ; arrest: 3.33 ± 0.29 , $p < 0.0001$).

180 **Figure 3. Kidney, Neurologic, and Serum Chemistry 1-day after SCA.** A) Percentage of mice with
181 recovered kidney perfusion over time since arrest ($n=10$). Mean recovery time was 20.55 ± 0.68 min. B)
182 SCA mice have increased kidney damage by semi-quantitative scoring of kidney injury in the outer
183 medulla ($n=5$ /group). C) Representative H&E stains of sham (top) and arrest (bottom) mice one-day after
184 arrest demonstrating proteinaceous casts in renal tubules (black arrowhead) and infiltrates (red
185 arrowheads) with glomeruli marked (blue asterisk). D) Elevated serum creatinine and BUN in SCA mice at
186 one-day. E) Neurologic scoring at one day. F) ALT, CK, and lactate changes at one day. Data are
187 expressed as mean +/- SEM. P-values: * < 0.05 , ** < 0.01 , *** < 0.001 , **** < 0.0001 .

188 **SCA mice have diffuse tissue injury at one day**

189 To assess systemic damage, additional serum assays were performed at 1 day to evaluate for liver
190 damage (ALT), muscle damage (CK), tissue ischemia (lactate), and neurologic function. These assays
191 were notable for a significant increase in ALT (sham: 47.6 ± 4.7 U/L; arrest: 135.6 ± 37.3 U/L, $p = 0.047$;
192 Figure 3) in arrest mice compared to sham. No significant changes were noted to serum CK (sham:
193 1244 ± 252 U/L; arrest: 1811 ± 570 U/L, $p = 0.36$) or normalized serum lactate (sham: 1.00 ± 0.06 ; arrest:
194 1.90 ± 0.64 , $p = 0.15$). Brief neurologic testing was performed as previously reported¹¹ on 14 sham and 17
195 arrest mice one day after SCA (Table 2). Two of the arrest mice were noted to have hind-leg ataxia and
196 one mouse had sluggish movement; however, there was no significant difference in neurologic testing
197 between the groups (sham: score 12.0 ± 0 ; arrest: score 11.8 ± 0.1 , $p = 0.13$; Figure 3).

198 **Table 2. 12-point Neurologic Function Assessment for One-Day Sham and SCA Mice**

Neurological Function	
Level of Consciousness	
No Tail Pinch Reflex	0
Weak Tail Pinch Reflex	1
Normal Tail Pinch Reflex	2
Corneal Reflex	
No Blink	0
Delayed Blink	1
Normal Blink	2
Respiration	
Irregular	0

Decreased Frequency with Normal Pattern	1
Normal Frequency and Pattern	2
Righting Reflex	
No Righting	0
Sluggish Righting	1
Rapid Righting	2
Coordination	
No Movement	0
Some Ataxia	1
Normal Coordination	2
Activity	
No Spontaneous Movement	0
Sluggish Movement	1
Normal Movement	2
Total Possible Score	12

199

200 **Discussion**

201 In this study, we modified the mouse model of SCA described by Hutchens et al.⁹ by delivering KCl
202 directly into the LV cavity under ultrasound guidance rather than IJ cannulation. This delivery method
203 causes immediate onset of asystole after KCl delivery in a highly controlled, easily visualized, and easily
204 adoptable manner. Pre-clinical models of SCA are rarely performed in the mouse despite a large number
205 of advantages of the murine model, including rapid development, low maintenance cost, and the
206 opportunity for genetic manipulation^{6,7}. The low utilization of the murine model is likely attributable to
207 surgical difficulties related to animal size. Groups that have embraced the mouse model of SCA almost
208 uniformly rely on intravenous delivery of KCl for induction of cardiac arrest, but have utilized various
209 durations of arrest (typically 4-16 minutes). These reports all use venous access either through the
210 jugular or femoral veins for drug delivery. Establishing reliable venous access in the mouse remains a
211 major barrier to wide-spread adoption of the mouse model of SCA.

212 Our model spares the use of major vessels for drug delivery by using direct LV introduction under
213 ultrasound, resulting in rapid procedure times, typically around 30 minutes from anesthesia induction to
214 extubation, with low surgical mortality (16.7% of SCA mouse surgical mortality, Table 1). Ultrasound-
215 guided catheter placement has already become a staple of hospital care for many clinicians, allowing
216 physicians and researchers to easily transfer a known skill set into a translational model of SCA^{18,19}.
217 Additionally, the destruction of major veins by cannulation in the traditional mouse model may limit

218 venous drainage post-operatively, which may affect both neurologic and cardiac performance. Our
219 method avoids both venous access and blockage. Further, ultrasound utilization allows for continual
220 non-invasive monitoring of cardiac function throughout the arrest, resulting in precise monitoring of
221 cardiac arrest duration. Previously published models that utilize only ECG as an indicator of ROSC may
222 falsely register pulseless electrical activity as a return of circulation, which may erroneously measure
223 ischemic duration. Other models utilize an LV pressure catheter to accurately record restoration of
224 cardiac flow; however, this requires the placement of an additional invasive canula. In the current
225 report, the rapid procedure time, high survival, reduced surgical skill required, and venous sparing by
226 this technique are highly advantageous over the traditional model.

227 Of the 30 mice that underwent arrest in this study, 25 survived the arrest and achieved ROSC, resulting
228 in a relatively low mortality rate (16.7%) for the procedure (Table 1). This is a modest improvement over
229 the 20% surgical mortality in the venous KCl mouse model described by Hutchens et al.⁹ and the 27%
230 mortality in a ventricular fibrillation mouse model described by Chen et al.⁸ A subset of mice was studied
231 for up to 4 weeks to assess long-term survival. At 72 hours, 6 of 13 arrest mice (46%) survived, which is
232 in line with comparable recent studies publishing between 10 and 45% survival at 72 hours²⁰⁻²². 5 of 13
233 mice (38%) survived for the entire duration of the study (Figure 1).

234 After one day, EF in SCA mice is significantly decreased from 59.9% at baseline to 39.9%. These values
235 are in-line with previously published one day EFs and are likely attributable to cardiac stunning²¹. EF
236 remains significantly decreased at one week (41.4%), with improvement at four weeks (49.8%, Figure 2).
237 These values and their relative improvement are similar to those observed in humans following cardiac
238 arrest in the absence of coronary disease, as evidenced by a case series of cardiac arrest survivors, which
239 noted 1 day EFs of 38%, 1 week EFs of 44%, and 2-3 week EFs of 50%²³.

240 Maintenance of body temperature is critically important to neurologic outcomes following SCA²⁴⁻²⁶. We
241 maintained body temperatures with active heating for 2 hours after arrest, but body temperatures fell
242 significantly after active heating was stopped, which is consistent with post-arrest changes in humans²⁷.
243 The SCA mice continued to show significant temperature dysregulation and depressed HR at one day
244 (Figure 1, Table 1). We were unable to demonstrate significant neurologic deficit 24 hours after arrest by
245 utilizing a well-established, 12-point examination¹¹. Delayed, spontaneous hypothermia is known to be
246 neuroprotective in other rodent cardiac arrest models and may explain the paucity of neurological injury
247 noted²⁸. We only noted ataxia in two mice and lethargy in one mouse following SCA, with no observable
248 deficits in sham mice. While some groups are able to demonstrate neurologic injury with as little as 6-
249 minutes of cardiac arrest²⁹, others have required extended arrest time of 12-14 minutes to detect
250 neurologic changes^{10,30}. The technique described in this paper would be easily modified to allow for
251 prolonged arrest time to study neurologic insult.

252 Mouse SCA models have been utilized to as a clinically-relevant model of both acute kidney injury^{31,32}
253 (one day after arrest) and chronic kidney disease (seven weeks after arrest, attributed to prolonged
254 inflammation after reperfusion)³². We show that our model of SCA similarly develops markers of AKI, as
255 evidenced by elevated serum creatinine, BUN, and tubular damage 1 day after arrest (Figure 3). Many of
256 the peripheral kidney tubules are anucleated one-day after arrest, which is a marker of nephrotic
257 damage in mice. Kidney injury is not typically apparent with 8 minutes of direct ischemia, which typically
258 require 15-20 minutes for the development of focal injury³³. By utilizing doppler ultrasonography of the
259 renal artery, we found that the kidney did not receive measurable perfusion until 11.25 minutes after

260 ROSC, for a total mean ischemia duration of 20.55 minutes, resulting in kidney ischemia times consistent
261 with established direct ischemia reperfusion injury models (Figure 3)^{34,35}.

262 Finally, our model suggests the presence of global ischemic injury following SCA. ALT, a non-specific
263 marker of liver injury, is significantly elevated one-day after SCA (Figure 3). However, there are non-
264 significant trends towards increased CK, a non-specific marker of muscle degradation, and serum lactate
265 levels in the SCA mice. These changes are consistent with the markers of secondary ischemic damage
266 seen in post-cardiac arrest patients. We anticipate that these changes could become significant with
267 prolonged arrest duration, but at the cost of increased mortality. Further evaluation of this multiple
268 organ damage and the degree to which each organ system is involved may be an important step toward
269 improving recovery and guiding post-cardiac arrest interventions.

270

271 **Conclusions**

272 We demonstrate a novel mouse model of SCA that utilizes direct LV injection of KCl under ultrasound
273 guidance that allows for rapid and reliable arrest with low surgical mortality. This model develops
274 significant cardiac, kidney, and liver injury at one day and a trend towards neurologic injury. Time of
275 injury but can be easily adapted to achieve neurologic insult. This model lowers the barrier to entry for
276 establishing a mouse model of SCA, which will help researchers investigate the mechanisms underlying
277 SCA mortality.

278

279 **References**

- 280 1. Benjamin EJ, Muntner P, Alonso A, et al. Heart Disease and Stroke Statistics — 2019 Update: A
281 Report From the American Heart Association. *Circulation*. 2019;139:e56-e528.
- 282 2. Daya MR, Schmicker RH, Zive DM, et al. Out-of-hospital cardiac arrest survival improving over
283 time: Results from the Resuscitation Outcomes Consortium (ROC). *Resuscitation*. 2015;91:108-
284 115.
- 285 3. Reynolds JC, Frisch A, Rittenberger JC. Out-of-Hospital Cardiac Arrest: When Should We Change
286 to Novel Therapies? *Circulation*. 2014;128(23):2488-2494.
- 287 4. Barouxis D, Chalkias A, Syggelou A, Iacovidou N, Xanthos T. Research in human resuscitation:
288 what we learn from animals. *J Matern Neonatal Med*. 2012;25(S5):44-46. d
- 289 5. Vognsen M, Fabian-Jessing BK, Secher N, et al. Contemporary animal models of cardiac arrest: A
290 systematic review. *Resuscitation*. 2017;113:115-123.
- 291 6. Vandamme TF. Use of rodents as models of human diseases. *J Pharm BioAllied Sci*. 2014;6(1):2-9.
- 292 7. Papadimitriou D, Xanthos T, Lelovas P, Perrea P. The Use of Mice and Rats as Animal Models for
293 Cardiopulmonary Resuscitation Research. *Lab Anim*. 2008;24:265-276.
- 294 8. Chen M, Liu T, Xie L, et al. A simpler cardiac arrest model in the mouse. *Resuscitation*.
295 2007;75:372-379.
- 296 9. Hutchens M, Traystman R, Fujiyoshi T, Nakayama S, Herson P. Normothermic Cardiac Arrest and
297 Cardiopulmonary Resuscitation: A Mouse Model of Ischemia-Reperfusion Injury. *Jove*. 2011;54.
- 298 10. Dezfulian C, Shiva S, Alekseyenko A, et al. Nitrite therapy after cardiac arrest reduces reactive
299 oxygen species generation, improves cardiac and neurological function, and enhances survival via
300 reversible inhibition of mitochondrial complex I. *Circulation*. 2009;120(10):897-905.
- 301 11. Abella BS, Zhao D, Alvarado J, Hamann K, Hoek TL Vanden, Becker LB. Intra-Arrest Cooling
302 Improves Outcomes in a Murine Cardiac Arrest Model. *Circulation*. 2004;109:2786-2791.
- 303 12. Ikeda K, Marutani E, Hirai S, Wood ME, Whiteman M, Ichinose F. Mitochondria-targeted
304 hydrogen sulfide donor AP39 improves neurological outcomes after cardiac arrest in mice. *Nitric
305 Oxide*. 2015;49:90-96.
- 306 13. Xu L, Zhang Q, Zhang QS, Li Q, Han JY, Sun P. Improved Survival and Neurological Outcomes after
307 Cardiopulmonary Resuscitation in Toll - like Receptor 4 - mutant Mice. *Chin Med J (Engl)*.
308 2015;128(19):1-6.
- 309 14. Rutledge C, Cater G, Mcmahon B, et al. Commercial 4-dimensional echocardiography for murine
310 heart volumetric evaluation after myocardial infarction. 2020;5:1-10.
- 311 15. Lang RM, Badano LP, Mor-avi V, et al. Recommendations for Cardiac Chamber Quantification by
312 Echocardiography in Adults : An Update from the American Society of Echocardiography and the
313 European Association of Cardiovascular Imaging. *J Am Soc Echocardiogr*. 2015;28(1):1-39.e14.
- 314 16. Chiba T, Peasley KD, Cargill KR, et al. Sirtuin 5 Regulates Proximal Tubule Fatty Acid Oxidation to
315 Protect against AKI. 2019;1-15.
- 316 17. Yanta J, Guyette FX, Doshi AA, et al. Renal dysfunction is common following resuscitation from

317 out-of-hospital cardiac arrest. *Resuscitation*. 2013;84(10):1371-1374.

318 18. Schmidt GA, Maizel J, Slama M. Ultrasound-guided central venous access : what's new? *Intensive*
319 *Care Med*. 2014;14-16.

320 19. Biasucci DG, La Greca A, Scoppettuolo G, Pittiruti M. What's really new in the field of vascular
321 access? Towards a global use of ultrasound. *Intensive Care Med*. 2015;10-12.

322 20. Id JL, Zhu X, Id HW, et al. Akt1-mediated CPR cooling protection targets regulators of metabolism,
323 inflammation and contractile function in mouse cardiac arrest. *PLoS One*. 2019;14(8):1-18.

324 21. Piao L, Fang Y, Hamanaka RB, et al. Suppression of Superoxide-Hydrogen Peroxide Production at
325 Site I. *Crit Care Med*. 2020;(1):133-140.

326 22. Piao L, Ph D, Varughese J, Archer SL. Inhibition of the Mitochondrial Fission Protein Drp1
327 Improves Survival in a Murine Cardiac Arrest Model. *Crit Care Med*. 2016;43(2):1-22.

328 23. Ruiz-bail M, Aguayo E, Hoyos D, et al. Reversible myocardial dysfunction after cardiopulmonary
329 resuscitation. 2005;66:175-181.

330 24. Abella BS, Zhao D, Alvarado J, Hamann K, Vanden Hoek TL, Becker LB. Intra-arrest cooling
331 improves outcomes in a murine cardiac arrest model. *Circulation*. 2004;109(22):2786-2791.

332 25. Nolan JP, Berg RA, Bernard S, et al. Intensive care medicine research agenda on cardiac arrest.
333 *Intensive Care Med*. 2017;43(9):1282-1293.

334 26. Sandroni C, Cavallaro F, Callaway CW, et al. Predictors of poor neurological outcome in adult
335 comatose survivors of cardiac arrest : A systematic review and meta-analysis . Part 2 : Patients
336 treated with therapeutic hypothermia. *Resuscitation*. 2013;84(10):1324-1338.

337 27. The Hypothermia After Cardiac Arrest Study Group. Mild Therapeutic Hypothermia to Improve
338 the Neurologic Outcome after Cardiac Arrest. *N Engl J Med*. 2002;346(8):549-556.

339 28. Hickey RW, Ferimer H, Alexander HL, et al. Delayed, spontaneous hypothermia reduces neuronal
340 damage after asphyxial cardiac arrest in rats. *Crit Care Med*. 2000;28(10):3511-3516.

341 29. Yong Y, Guo J, Zheng D, et al. Electroacupuncture pretreatment attenuates brain injury in a
342 mouse model of cardiac arrest and cardiopulmonary resuscitation via the AKT / eNOS pathway.
343 *Life Sci*. 2019;235:116821.

344 30. Kofler J, Hattori K, Sawada M, et al. Histopathological and behavioral characterization of a novel
345 model of cardiac arrest and cardiopulmonary resuscitation in mice. *J Neurosci Methods*.
346 2004;136(1):33-44.

347 31. Burne-taney MJ, Kofler J, Yokota N, et al. Acute renal failure after whole body ischemia is
348 characterized by inflammation and T cell-mediated injury. *Am J Physiol Ren Physiol*.
349 2003;285:F87-F94.

350 32. Matsushita K, Saritas T, Eiwaz MB, et al. The acute kidney injury to chronic kidney disease
351 transition in a mouse model of acute cardiorenal syndrome emphasizes the role of inflammation.
352 *Kidney Int*.:10-17.

353 33. Heyman SN, Rosen S, Rosenberger C. Animal models of renal dysfunction : acute kidney injury.
354 *Expert Opin if Drug Discov*. 2009;4(6):629-641.

355 34. Shanley PF, Rosen MD, Brezis M, Silva P, Epstein FH, Rosen S. Topography of focal proximal
356 tubular necrosis after ischemia with reflow in the rat kidney. *Am J Pathol*. 1986;122(3):462-468.

357 35. Glaumann B, Glaumann H, Berezesky IK, Trump BF. Studies on the pathogenesis of ischemic cell
358 injury. II. Morphological changes of the pars convoluta (P1 and P2) of the proximal tubule of the
359 rat kidney made ischemic in vivo. *Virchows Arch B, Cell Pathol*. 1975;19(4):281-302.

360

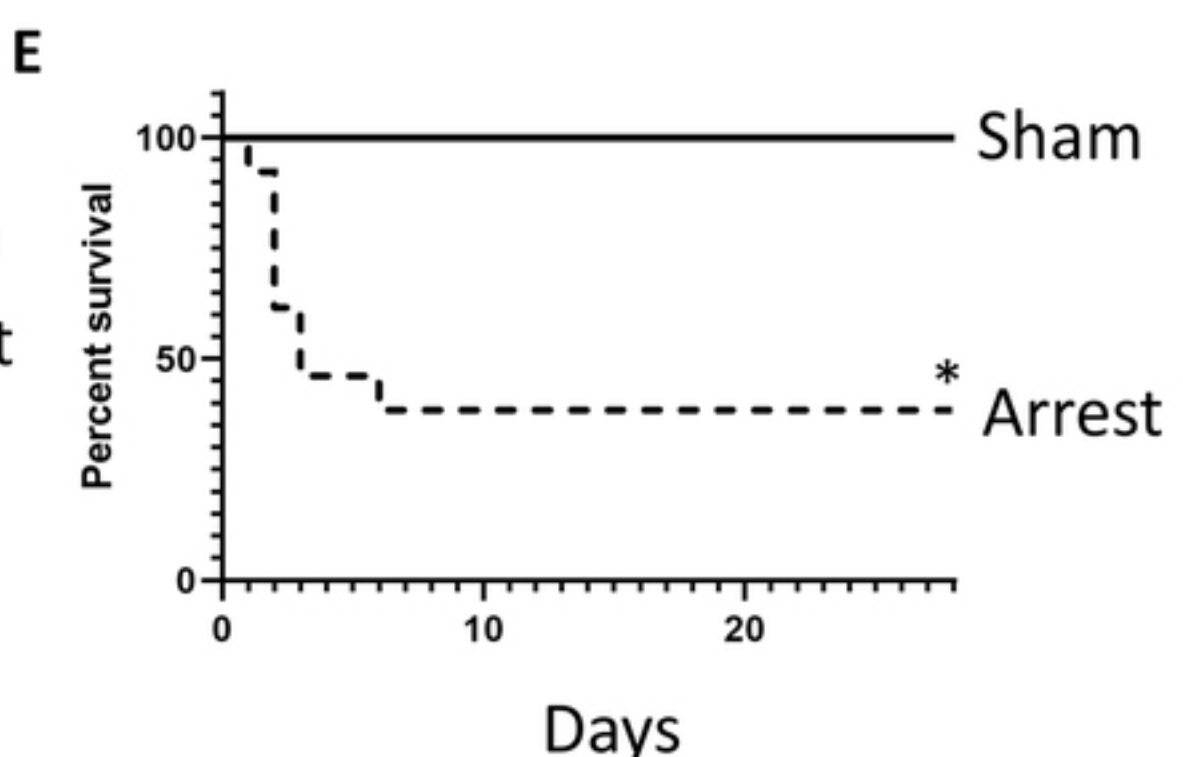
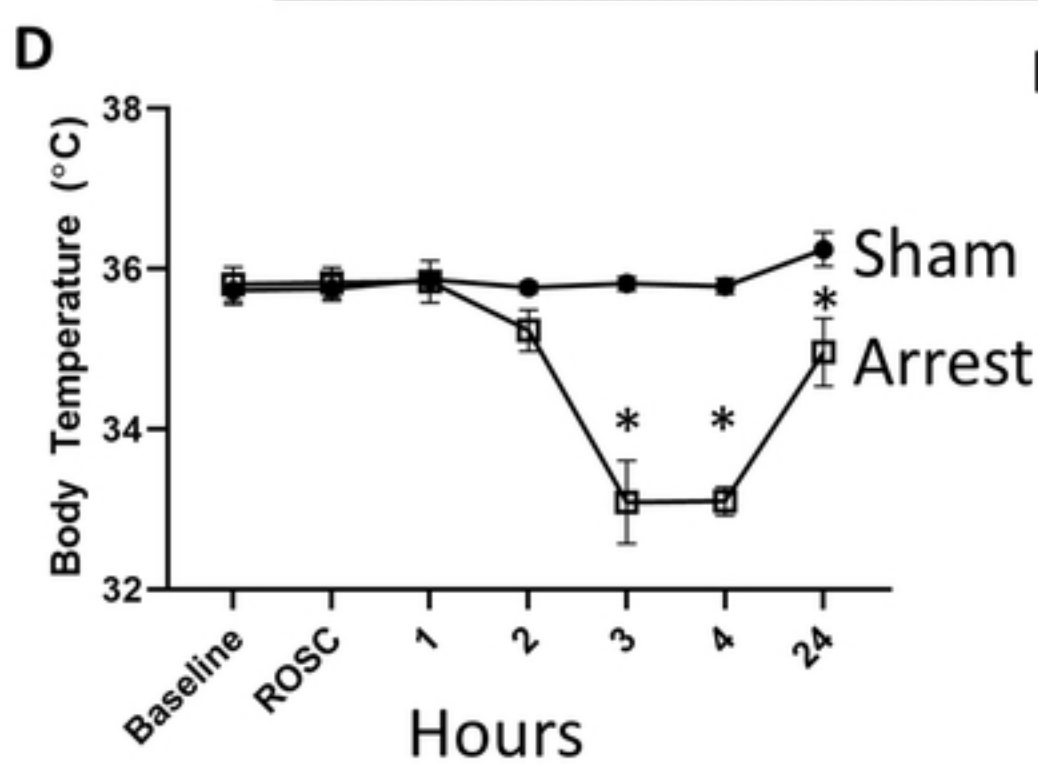
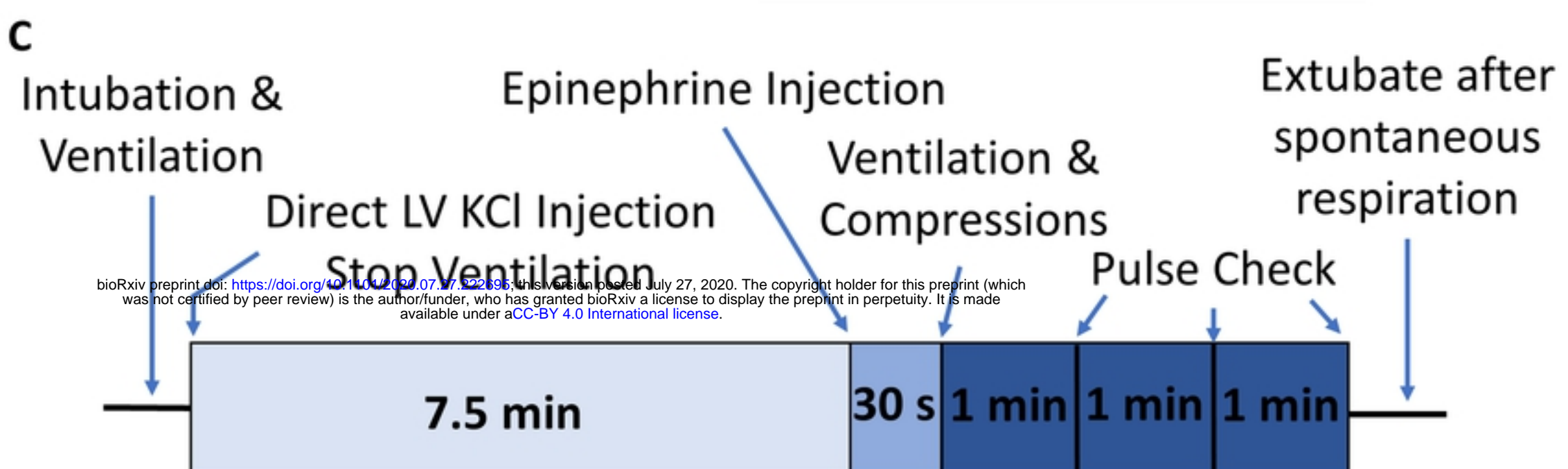
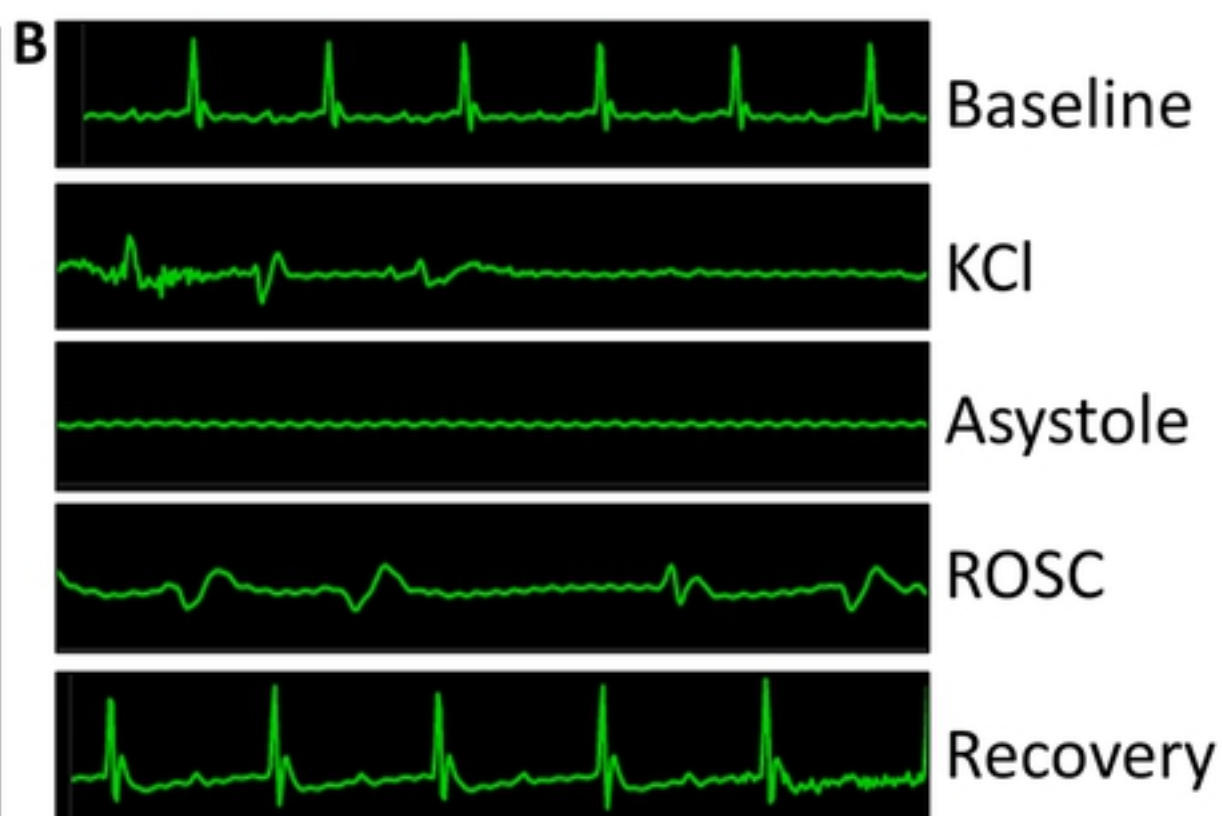
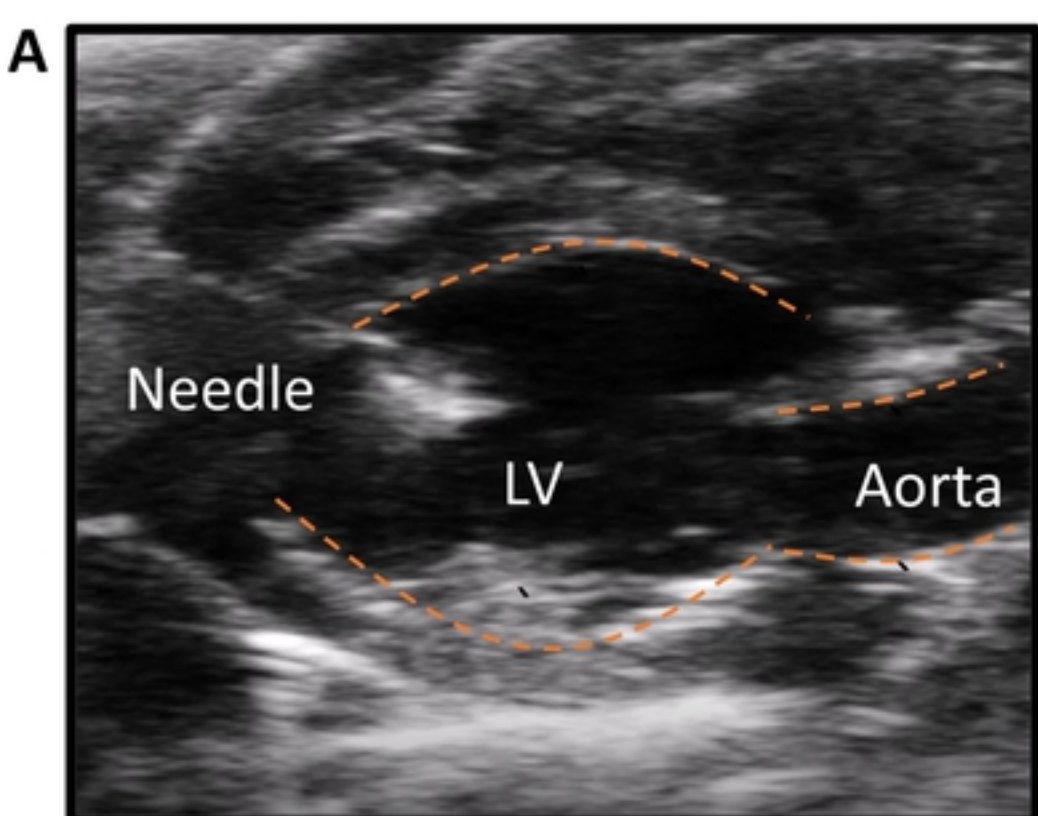


Figure 1

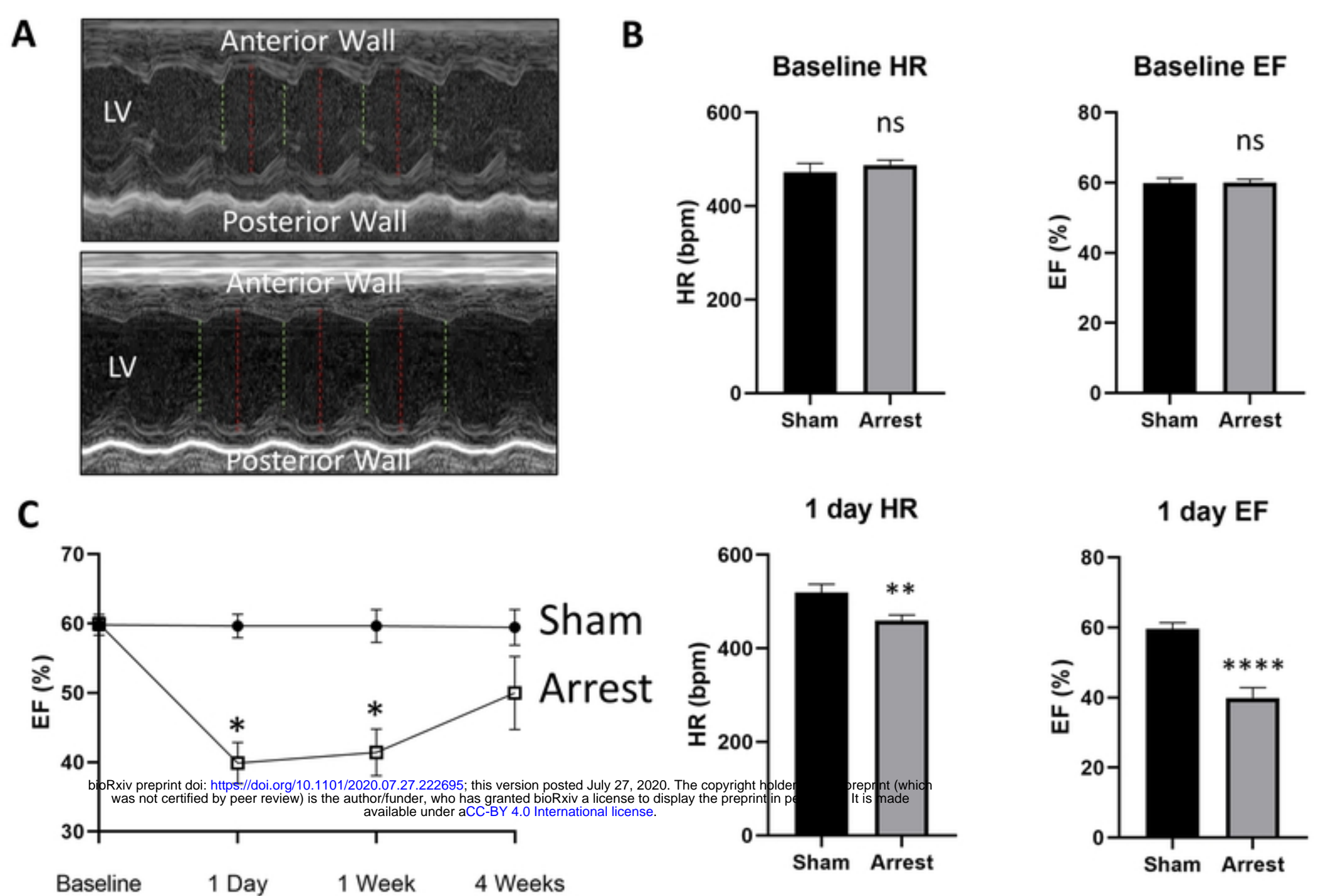


Figure 2

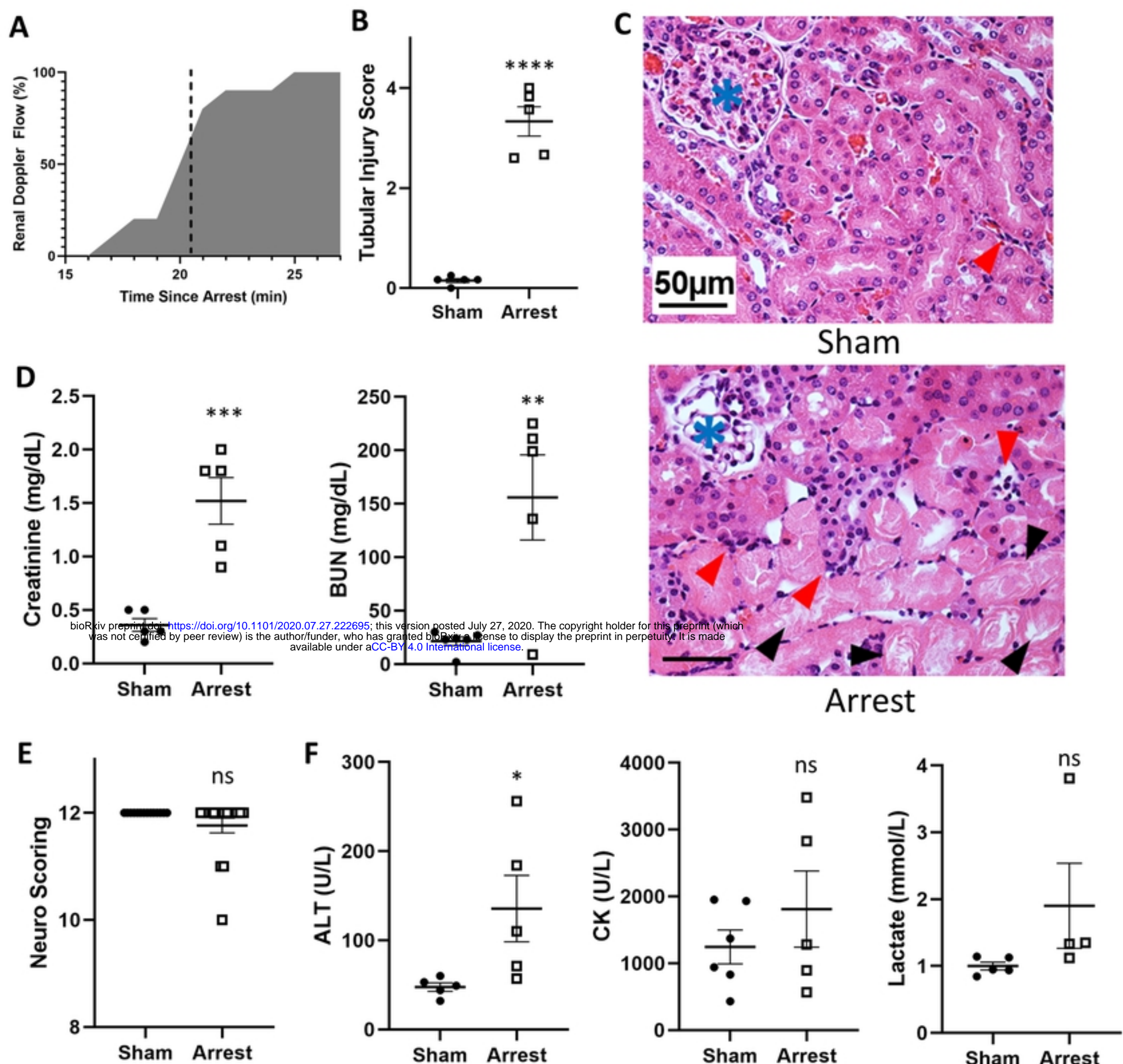


Figure 3